

PROJECT REPORT
on
MICROWAVE FILTERS
Submitted by

JOEL ROY - 20320037

in partial fulfillment of requirement for the award of the degree

of

BACHELOR OF TECHNOLOGY
in
ELECTRONICS AND COMMUNICATION



DIVISION OF ELECTRONICS ENGINEERING
SCHOOL OF ENGINEERING
COCHIN UNIVERSITY OF SCIENCE AND TECHNOLOGY
KOCHI-682022
APRIL 2023

DIVISION OF ELECTRONICS ENGINEERING
SCHOOL OF ENGINEERING
COCHIN UNIVERSITY OF SCIENCE AND
TECHNOLOGY KOCHI-682022



CERTIFICATE

*Certified that the seminar report entitled “ **MICROWAVE FILTERS** ” is a bonafide work of ALEENA MARIA GEORGE, AMRITA UNNI ,BASITHA A L, BHAGYALAKSHMI PA, JOEL ROY.... towards the partial fulfillment for the award of the degree of B.Tech in Electronics and Communication of Cochin University of Science and Technology, Kochi-682022.*

Project Coordinator

Dr. Abdullah .P

Head of the Division

Dr.Anju Pradeep

ACKNOWLEDGEMENT

We extend our heartfelt gratitude to all those who have contributed to the successful completion of this project on "Microwave Filters." This endeavor would not have been possible without the support, guidance, and encouragement of various individuals and organizations. We would like to express our deepest appreciation to Dr. Abdulla P, our project supervisor, for providing invaluable guidance throughout the research process. Your expertise and insightful feedback have been instrumental in shaping the direction and quality of this project. We are thankful to the faculty members of Department of Electronics and Communication for their continuous support and encouragement. Special thanks to Parvathy for sharing your expertise in microwave engineering and offering valuable suggestions that enhanced the depth of our understanding. We are also grateful to our peers and fellow students who have been a constant source of inspiration and collaboration. The exchange of ideas and discussions have enriched our perspective and contributed to the overall improvement of this project. Furthermore, we would like to acknowledge the resources and facilities provided by School of Engineering, CUSAT that facilitated the smooth progress of this research. The well-equipped laboratories and access to relevant literature have been crucial in conducting experiments and gathering essential data. Last but not least, we want to express our gratitude to our family and friends for their unwavering support and encouragement throughout this academic journey. Your belief in our abilities has been a driving force behind the successful completion of this project.

Thank you to everyone who has played a role, big or small, in making this project a reality.

ABSTRACT

Microwave filters are key elements in microwave and RF engineering, serving as critical components in communication systems, radar systems, and various wireless applications. These filters are designed to manipulate the spectral characteristics of signals by allowing desired frequencies to pass through while attenuating unwanted frequencies. The demand for efficient and compact filters has led to the development of diverse filter topologies, including cavity filters, microstrip filters, and lumped element filters. Advanced materials and fabrication techniques are employed to achieve optimal performance in terms of insertion loss, bandwidth, selectivity, and size. Microwave filters find applications in satellite communication, cellular networks, radar systems, and scientific research. Different filter architectures, such as cavity filters, microstrip filters, and lumped element filters, are employed based on the specific requirements of the application. microstrip filters utilize printed circuit board technology, enabling compact and lightweight designs that are well-suited for modern wireless communication devices. Lumped element filters, which consist of discrete components like inductors and capacitors, offer flexibility in design but may be limited in terms of size and frequency range.

CONTENTS

Title	Page No.
List of Figures	1
List of Table	1
Chapter 1	2
Chapter2	4
Chapter3	14
Chapter4	18
References	19
Appendix	20

LIST OF FIGURES

CHAPTER 1

INTRODUCTION

In the dynamic landscape of telecommunications and scientific research, the role of Microwave, Gigahertz (GHz), and Terahertz (THz) filters stands as paramount. These filters serve as critical elements in signal processing, enabling the manipulation of electromagnetic waves across a vast spectrum of frequencies. This report endeavors to provide a succinct yet comprehensive exploration of these filter technologies, delving into their principles, applications, and recent advancements. Microwave filters, operating within the GHz range, are indispensable in radar systems, satellite communications, and wireless networks. Leveraging resonant cavities, transmission lines, and waveguides, they selectively attenuate or pass specific frequencies, facilitating efficient signal processing. Gigahertz filters, optimized for frequencies ranging from 1 GHz to 30 GHz, play a crucial role in high-speed data transmission and wireless communications. They employ similar principles to microwave filters but are tailored to tighter tolerances and higher frequencies, supporting the demands of modern telecommunications infrastructure. Terahertz filters, operating within the 0.1 THz to 10 THz range, bridge the gap between microwave and infrared frequencies, enabling groundbreaking applications in imaging, spectroscopy, and high-speed communications. Exploiting phenomena such as plasmonics, photonic crystals, and quantum effects, they offer unprecedented control over electromagnetic waves in the THz spectrum. Recent advancements in filter technology focus on enhancing bandwidth, miniaturization, and integration. Techniques such as metamaterials, reconfigurable filters, and graphene-based filters promise to revolutionize filter design, unlocking new possibilities for future wireless and optical technologies. The Terahertz (THz) range spans frequencies between 0.1 THz to 10 THz, corresponding to wavelengths ranging from 30 micrometers to 3 millimeters. This range sits between the microwave and infrared regions of the electromagnetic spectrum. On the other hand, the Gigahertz (GHz) range covers frequencies between 1 GHz to 30 GHz, with wavelengths ranging from 30 centimeters to 1 centimeter. This range falls within the microwave portion of the electromagnetic spectrum and is commonly used in various wireless communication systems, radar applications, and scientific research.

Applications of microwave filters:

Microstrip filters are utilized in various applications, including:

- **Communication Systems:** Microstrip filters play a crucial role in wireless communication systems,

including cellular networks, Wi-Fi, and satellite communication. -

- Radar Systems: Radar systems use microstrip filters for signal processing and frequency selection. -
- Medical Imaging: Microstrip filters are employed in medical devices, such as MRI machines and communication systems in healthcare applications.
- Aerospace and Defense: Microstrip filters are commonly used in avionics and defense applications for their reliability and performance.

CHAPTER 2

DESIGN AND WORKING

i) Dual split resonator lowpass filter with ultrawide stopband and sharp roll-off rate

Conventional constructions of split resonators are by using concentric rectangular loop split rings. Here split resonators (SR-1 and SR-2) with dual splits (DSR-1 and DSR-2) are designed on a substrate with a thickness of 0.79 mm, the loss tangent of 0.0009 and a dielectric constant of 2.2 to obtain better coupling and achieve maximum frequency performance.

ii)Capacitively-Coupled Resonators for Terahertz Planar-Goubau-Line Filters

The substrate is characterized by a bulk permittivity of $\epsilon_r = 11.7$ and a low tangent loss ($\tan \delta = 1.7 \times 10^{-5}$), was chosen for its capacity to minimize dielectric and radiation losses critical at THz frequencies. The use of gold as a conductor ($\sigma = 4.1 \times 10^7$ S/m) further ensures high conductivity and low losses in the filter structure. The design of the planar Goubau line (PGL) involved optimizing key parameters to achieve optimal performance while mitigating losses. A relatively large strip width of $w_p = 10 \mu\text{m}$ which decreases conductor loss. For the resonator width and gap we took $w_r = 5 \mu\text{m}$ and $g_r = 5 \mu\text{m}$ to guarantee subwavelength structure and operate well below the Bragg frequency. A coupling gap of $g_c = 10 \mu\text{m}$ is chosen. Port sizes were a vacuum wavelength at the lowest frequency of analysis for PGL and resonators, and $3(w_p + 2g_c)$ by $2(w_p + 2g_c)$ for the rectangular port for the coplanar waveguide.

iii).Design of THz low pass filter using split-ring resonators

A Polyimide substrate with thickness=1.6 μm and bulk permittivity of 3.5 and loss tangent of 0.0027 is chosen. The design process involves calculating the transmission line equivalent of the SRR using the parameters of inductors and capacitors with electromagnetic coupling linking the two concentric rings. The resonance of the SRR witnesses the permittivity being negative, thereby producing a clean rejection stopband.

iv).Improved Frequency Response of Microstrip Lowpass Filter Using Defected Ground Structures

A series resonant branch having a high impedance stub and a low impedance patch, modeled as inductor and

capacitor respectively, is connected in shunt with a high impedance main transmission line. The dimensions are $l_1 = 6.4$ mm, $l_2 = 4$ mm, $l_3 = 3.6$ mm, $w = 0.2$ mm and $w_1 = 3.6$ mm. The high impedance main transmission line of length l_1 is represented as ZL_1 and the impedance of the series resonant branches are ZL_2 and ZC_1 respectively. The width, w_0 , of the microstrip line is chosen to be 1.5 mm which corresponds to the characteristic impedance of 50Ω . All simulations are carried out using full wave EM simulator CST and the substrate used is FR4 with relative dielectric constant 4.4, thickness $h = 0.8$ mm and dielectric loss tangent 0.02. A one-pole microstrip lowpass filter with an H-shaped slot etched on the metallic ground plane is simulated. In order to analyze the frequency characteristics of the DGS section, the structure is simulated with CST software. The dimensions of the DGS unit are $a = 7.1$ mm, $b = 1.6$ mm, $c = 1.8$ mm, $d = 2.2$ mm and $w_0 = 1.5$ mm.

CHAPTER 3

IMPLEMENTATION AND DEVELOPMENT

3.1.FILTERS IN GIGAHERTZ RANGE

3.1.1) Dual split resonator lowpass filter with ultrawide stopband and sharp roll-off rate

After the detailed survey of SRR, CSRR and other approaches, the design procedures are found to be common and by using the SRR with different geometry etched in the ground plane. The splits in the geometry of resonators can make a difference in the performance characteristics of the filters and the proposed resonators can replace the other SRR for the enhancement in the filter response. The more complex approaches in the field of filter design are replaced by the proposed design using dual split resonator (DSR) to attain the maximum frequency performances. Here dual splits are introduced in the rectangular loop resonator which provides simultaneous advancement in the roll-off rate of 224 dB/GHz at 30 dB suppression and stopband up to 25 GHz with a passband insertion loss <0.1 dB at lower frequencies. The details of resonator structures used in this filter are given below.

i.)Dual split resonator-1 (DSR-1)

Splits on both sides of a rectangular loop with low impedance patch, which are placed on the high impedance stub constitute DSR-1 shown in Fig. 1a. Here a_0 denotes the splits in the rectangular loop and a_5 gives the low impedance patch with $Z_{C1} = 38.83 \Omega$. The loop having splits on both sides are placed on high impedance stub showing a_1 and having characteristic impedance of $Z_{L1} = 159.03 \Omega$. The capacitive element 'CSRC' connected to the high impedance stub with inductance in DSR-1 is expanded into the combination of short-circuited stub inductances and capacitances. This approach shows the effect of coupling capacitance in the circuit and also agrees with the EM simulation results even though the elements within the CSRC in DSR-1 have a capacitive nature.

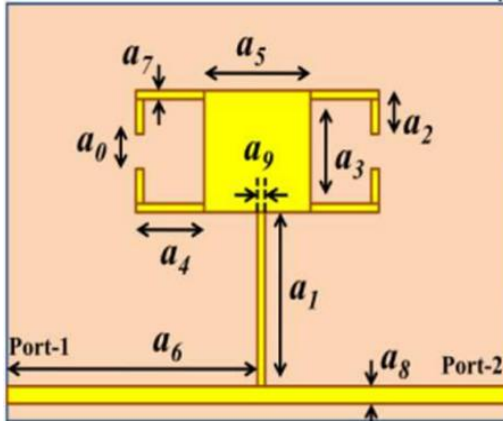


Fig:1 DSR1

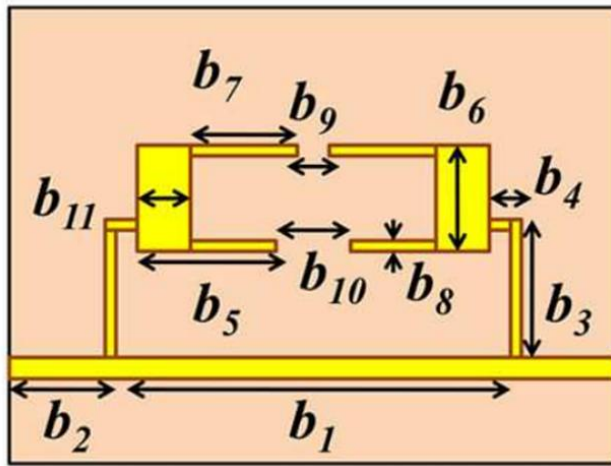
Dimensions of DSR-1	
Parameters	Values, mm
a_0	0.75
a_1	2.7
a_2	0.75
a_3	1.85
a_4	3
a_5	3.5
a_6	11.4
a_7	0.2
a_8	0.5
a_9	0.2

Table 1: Dimensions of DSR1

The 3 dB cutoff frequency is at 2.5 GHz and DSR-1 resonates at 4.3 GHz .

ii.)Dual split resonator-2 (DSR-2)

The rectangular loop resonator has an asymmetrical thickness and dual splits on top and bottom form DSR-2. It is placed on a bent high impedance stub shown in Fig. 3a. The DSR-2 is a rectangular loop with low impedance patch on both sides which is indicated using capacitance C_{b6} and the coupling within the center splits connects the orientation of both resonators. Physical parameters and the designed equivalent circuit element values for the single DSR-2 are given in Table 2. The proposed DSR-1 and DSR-2 are not regular-shaped structures and EM simulations are encountered with some parasitic effects along with dielectric losses and conductor losses as it comes to the substrate material . The DSR-2 having resonators designed on both sides achieves two resonances f_{z1} and f_{z2} with 35 and 65 dB attenuation, respectively.



Dimensions of DSR-2	
Parameters	Values, mm
b_1	10.6
b_2	6
b_3	3.5
b_4	0.5
b_5	4.7
b_6	3.2
b_7	3.15
b_8	0.2
b_9	0.2
b_{10}	0.6
b_{11}	1.75

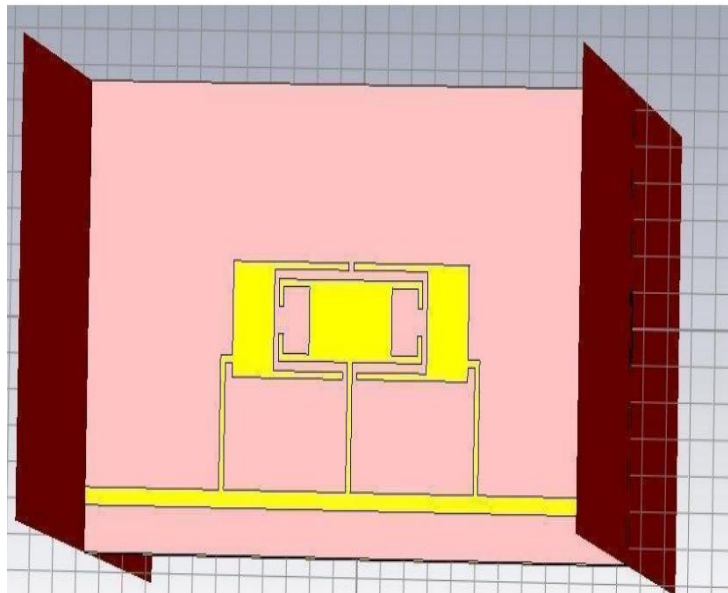
Fig:3.DSR2

Table 2: Dimensions of DSR2

The circuit analysis of DSR-2 is complex as it involves two transmission zeros using two symmetrical resonators separated by dual splits. The transmission zero at 3.5GHz and 4.8 GHz are achieved.

iii) Analysis of cascaded DSR structure

The DSR structure placed in parallel, on the high impedance transmission line will decrease the effective impedance of the resonator circuit. It also provides further suppression at the stopband and widens the region beyond cut-off frequency as shown in fig below.



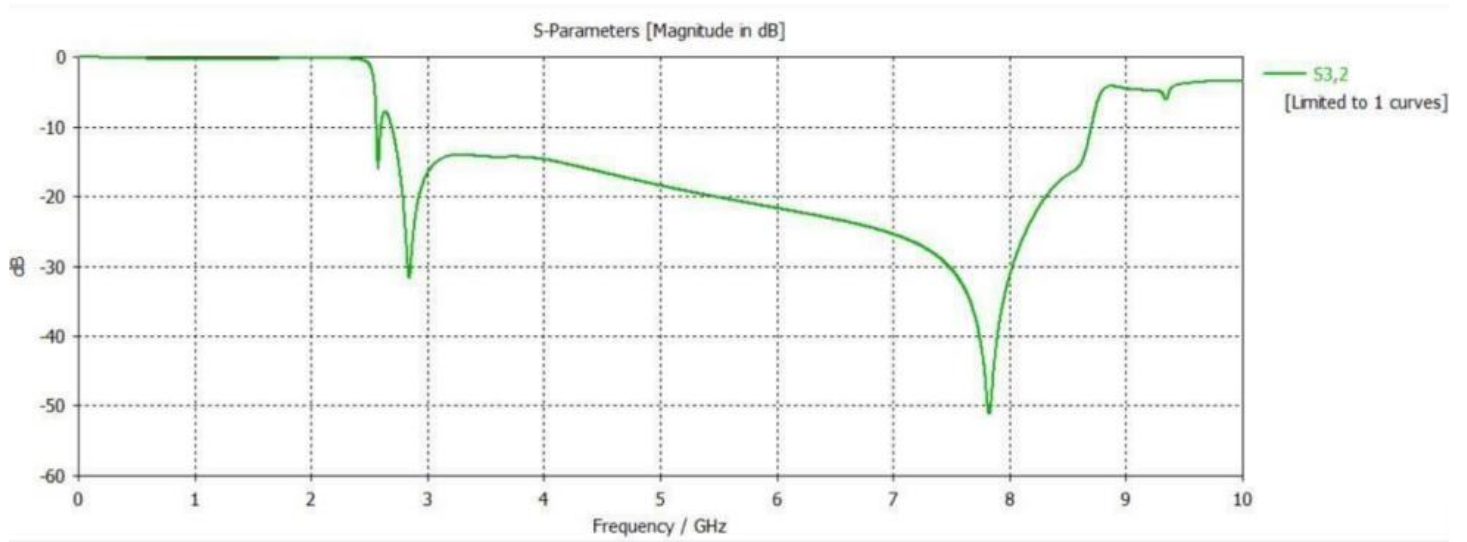


Fig.6.Simulation results of Cascading DSR1 and DSR2

Stop Band is from 2.8GHz to 7.8 GHz

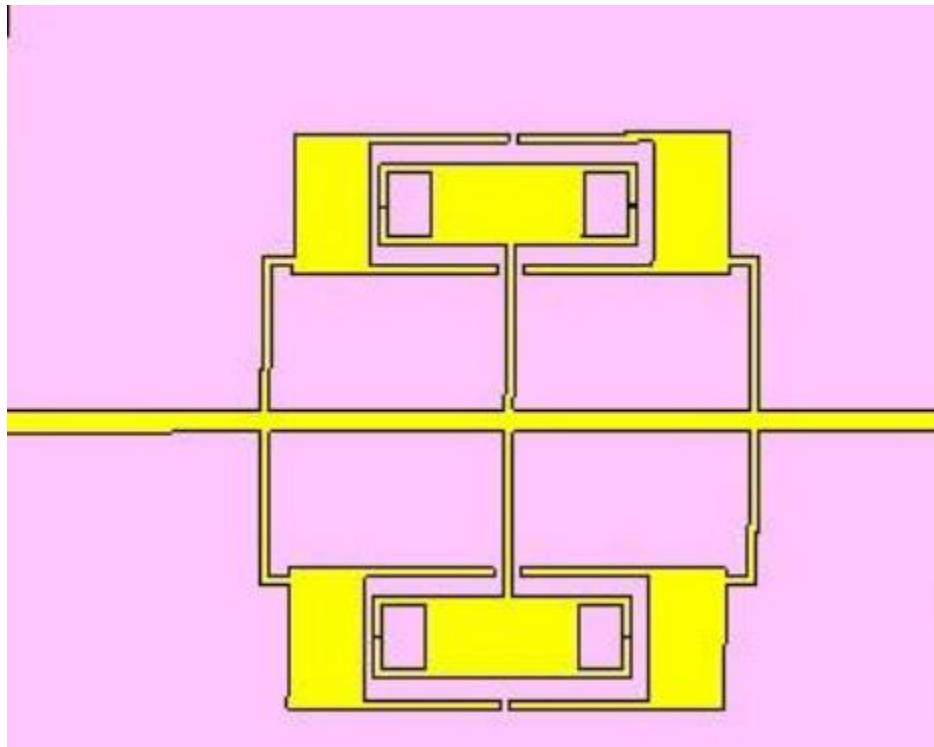


Fig.7.Parallely Cascading DSR1 and DSR2

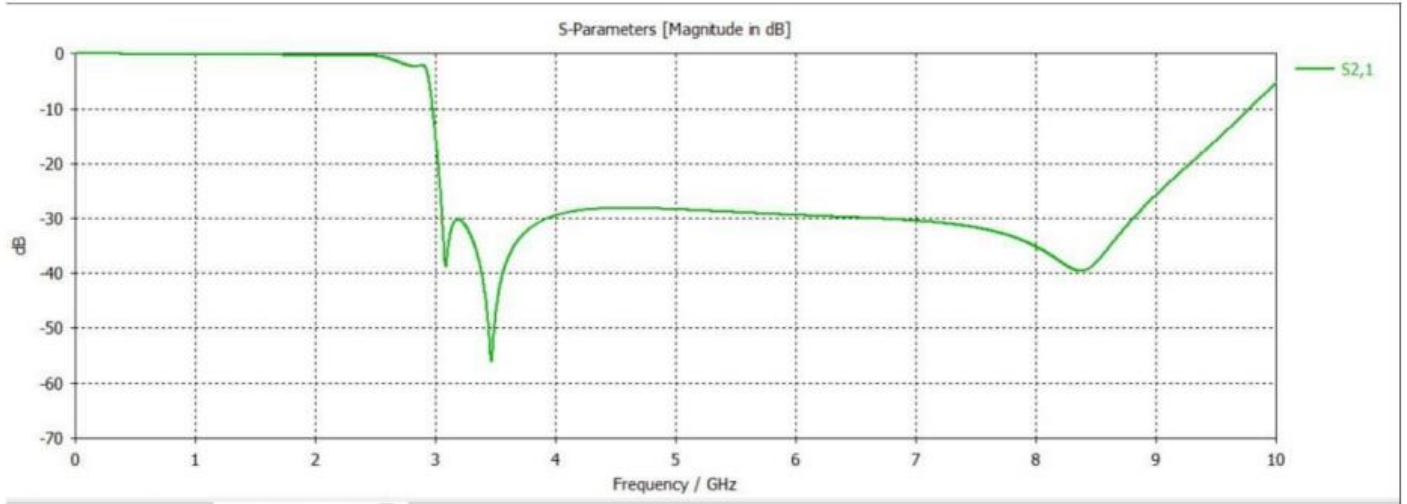


Fig:8.. Simulation results of parallel cascade DSR1 and DSR2

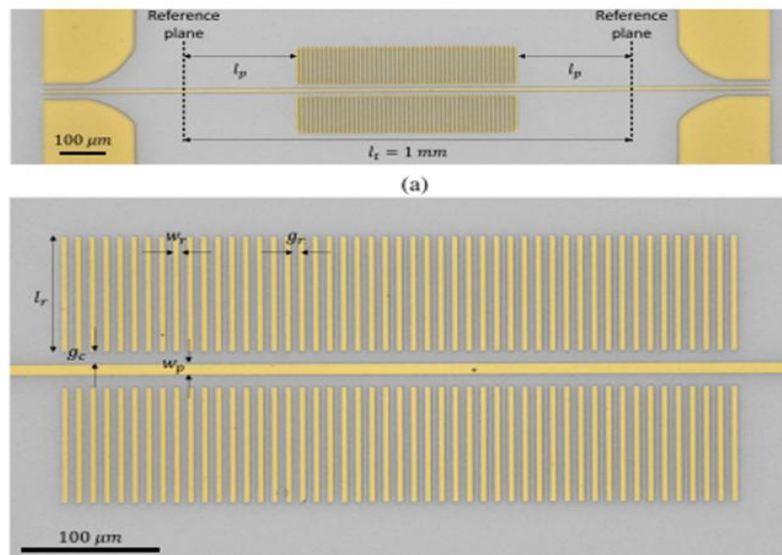
Shift in Stopband from 3.5 GHz to 8.5GHz.

2.2.FILTERS IN TERAHERTZ RANGE

Capacitively-Coupled Resonators for Terahertz Planar-Goubau-Line Filters

The proposed terahertz (THz) filter design comprises a planar Goubau line (PGL) periodically loaded with capacitively-coupled $\lambda/2$ resonators arranged in a balanced configuration. Physically separated from the PGL to avoid short-circuiting its propagating mode, these resonators are positioned in close proximity to induce coupling with the PGL. The shunt resonators introduce an input impedance along the line, generating stopbands in the frequency response when their impedances approach a short circuit. To enhance the bandwidth of these stopbands and produce sharper, narrower passbands, the filter adopts a periodic structure comprising N equal resonator pairs in cascade. The layout parameters of the filter, including the PGL's width (w_p), resonator's length (l_r), gap (g_r), and width (w_r), as well as the line-resonator coupling gap (g_c), are meticulously optimized to achieve the desired performance.). The substrate is characterized by a bulk permittivity of $\epsilon_r = 11.7$ and a low tangent loss ($\tan \delta = 1.7 \times 10^{-5}$), was chosen for its capacity to minimize dielectric and radiation losses critical at THz frequencies. The use of gold as a conductor ($\sigma = 4.1 \times 10^7$ S/m)

further ensures high conductivity and low losses in the filter structure. The design of the planar Goubau line (PGL) involved optimizing key parameters to achieve optimal performance while mitigating losses. A relatively large strip width of $w_p = 10 \mu\text{m}$ was chosen for the PGL to minimize conductor loss. Additionally, resonator width (w_r) and gap (g_r) were set to $5 \mu\text{m}$ each to ensure a subwavelength structure and operate comfortably below the Bragg frequency. A coupling gap (g_c) of $10 \mu\text{m}$ was selected to facilitate coupling between the resonators without short-circuiting the line's propagating mode. Electromagnetic simulations of a single resonator pair of arbitrary length were compared with the model, demonstrating fair agreement and replicating resonances in transmission. Subsequent analysis of the filter's transmission characteristics revealed an increase in stopband bandwidth with the number of unit cells, saturating around 20. A total of 49 unit cells were selected for the filter to optimize performance.



ii).Improved Frequency Response of Microstrip Lowpass Filter Using Defected Ground Structures.

The frequency response characteristics of a basic microstrip lowpass filter improved using H-shaped defected

ground structures are presented. The proposed defected ground structures behave as a resonant element at high frequency and thus eliminate the stopband frequencies to achieve wide stopband rejection. The 3 dB cutoff frequency of the filter is 1.935 GHz. Due to the defects etched in the ground plane of the basic structure, the harmonic rejection is improved from 5th to 10th order along with low insertion loss and voltage standing wave ratio together with good selectivity. The compact filter has a size of $0.0338\lambda_g$, with $\lambda_g = 85.18$ mm being the guided wavelength at the cutoff frequency. The characteristics of the lowpass filter are verified through simulation and measurement. Consistent and stable results are obtained. Conventional lowpass filter design using SIR-UIS has the capability to generate transmission zeros at their resonant frequencies. To obtain a wider stopband, more elements have to be added which will naturally increase the physical size of the filter. Here, a basic microstrip lowpass filter is designed using SIR-UIS to achieve the desired characteristics. Before going into the basic filter design, a primary resonator is analyzed. A series resonant branch having a high impedance stub and a low impedance patch, modeled as inductor and capacitor respectively, is connected in shunt with a high impedance main transmission line as shown in Figure 1(a). The dimensions are $l_1 = 6.4$ mm, $l_2 = 4$ mm, $l_3 = 3.6$ mm, $w = 0.2$ mm and $w_1 = 3.6$ mm. The high impedance main transmission line of length l_1 is represented as ZL1 and the impedance of the series resonant branches are ZL2 and ZC1 respectively. The width, w_0 , of the microstrip line is chosen to be 1.5 mm which corresponds to the characteristic impedance of 50Ω . The substrate used is FR4 with relative dielectric constant 4.4, thickness $h = 0.8$ mm and dielectric loss tangent 0.02. The cutoff frequency of the microstrip implementation of the structure is 2.13 GHz, and the single transmission zero occurs at 2.916 GHz. By using the same idea, the primary resonator is extended to the basic microstrip lowpass filter design using SIR-UIS to obtain a wide stopband up to 9.874 GHz at 20 dB suppression level, shown in Figure 2(a). The structure consists of two uniformly shaped low impedance stubs and three stepped impedance resonators, Resonator-1, Resonator-2 and Resonator-3 loaded on the high impedance main transmission line. The uniformly shaped low impedance stubs can be modeled as a capacitor, having width and length l_0 and w_0 respectively. The three stepped impedance resonators have a high impedance line loaded by low impedance square and rectangular patches as represented in Figure 2(a). The dimensions of the layout are $w = 0.2$, $w_1 = 3.6$, $w_2 = 3.7$, $w_3 = 4.05$, $w_0 = 1.15$, $l_1 = 2.8$, $l_2 = 3.8$, $l_3 = 0.9$, $l_4 = 3.6$, $l_5 = 6.05$, $l_6 = 3.6$, $l_7 = 3.05$, $l_8 = 3.6$, $l_9 = 3.0$, $l_{10} = 4.55$, $l_0 = 13.0$ (all in mm). The frequency response of the basic lowpass filter is shown in Figure 2(b). The cutoff frequency of the filter is 1.95 GHz, and the frequency at 20 dB suppression level is 2.464 GHz. The selectivity of the filter is 33.36 dB/GHz. The insertion loss is less than 0.35 dB up to 1.1 GHz of the passband, and the return loss in the passband is better than 14.7 dB. The stopband bandwidth at 20 dB suppression level is from 2.464 GHz to 9.874 GHz, and the relative stopband bandwidth (RSB) calculated as a

percentage (the ratio of stopband bandwidth to stopband centre frequency) is 120.1%. The physical size of the filter is only $15.1 \text{ mm} \times 14.95 \text{ mm}$. The main drawback of this filter is the presence of out of band spurious frequencies. To improve the performance, these components have to be suppressed, without increasing the physical size. DGS is an appropriate choice due to its attractive features such as simplicity, wide and deeper stopband characteristics. To improve the performance of the basic lowpass filter without compromising the size, defected ground structures are used to design the proposed filter, Filter-1. It is the same SIR-UIS structure with two symmetrical H-shaped slots etched on the ground plane. The size and shape of DGS are selected such that it should resonate at a higher frequency so as to extend the stopband bandwidth of the basic structure.

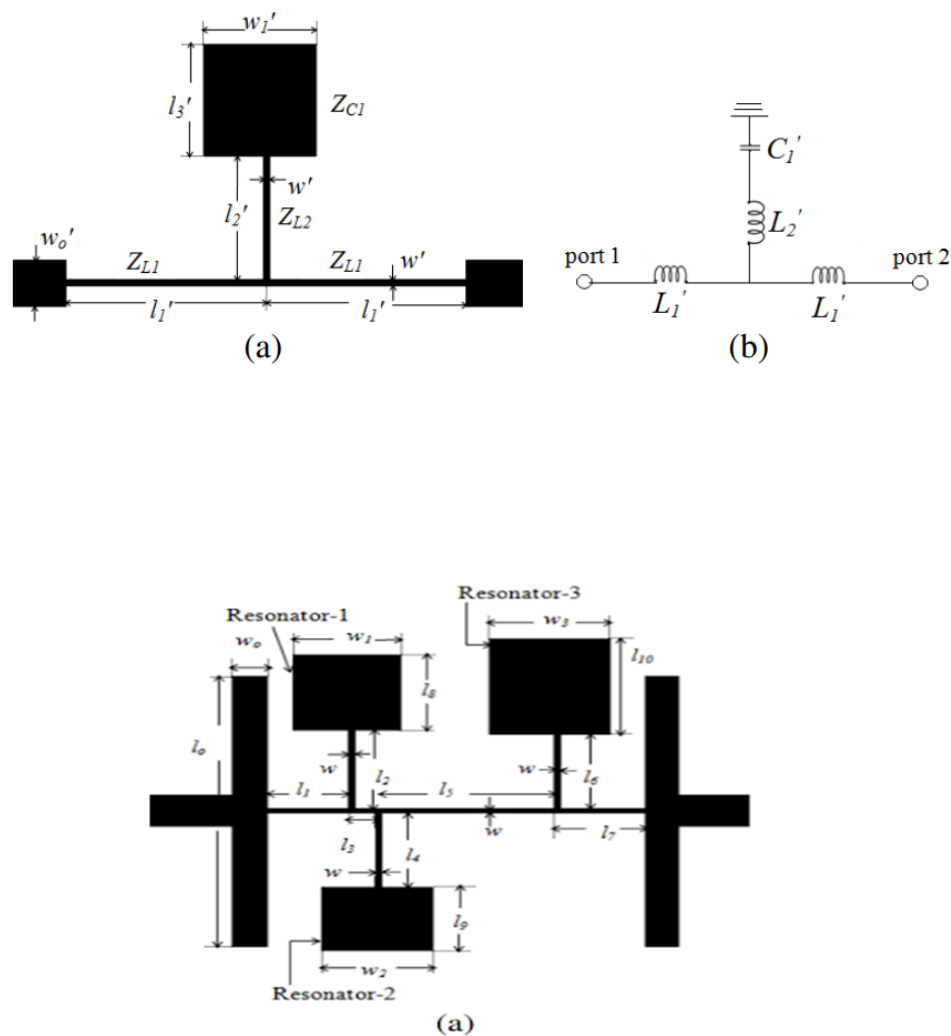
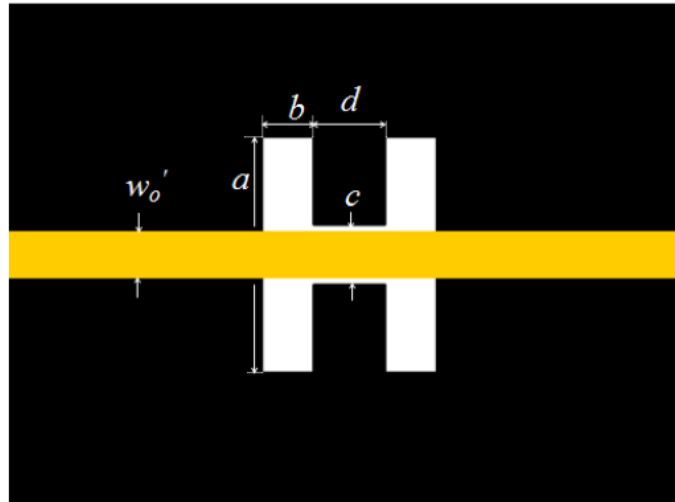


Figure 2. (a) Layout of the basic lowpass filter

Characterstics of H-Shaped DGS

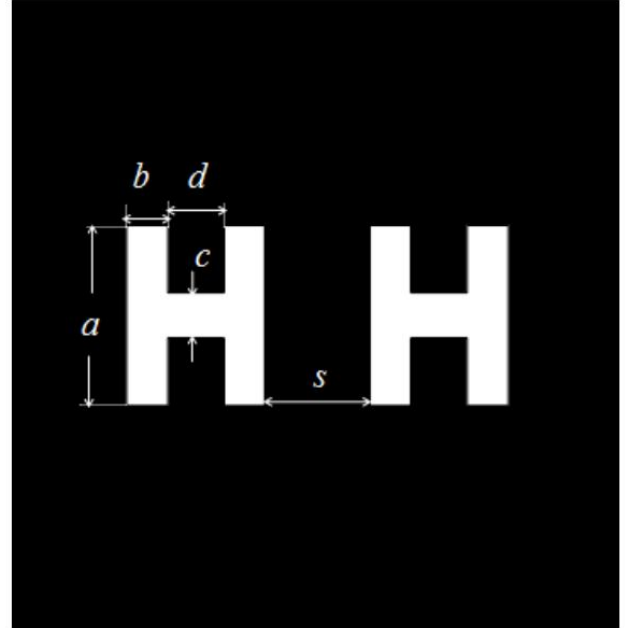
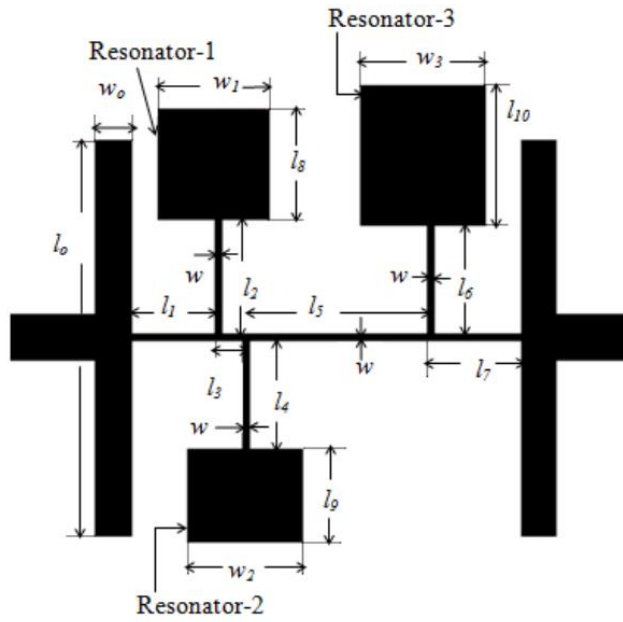
A one-pole microstrip lowpass filter with an H-shaped slot etched on the metallic ground plane is analyzed, and its structure is shown in Figure 3(a). In order to analyze the frequency characteristics of the DGS section, the structure is simulated with CST software. The dimensions of the DGS unit shown in Figure 3(a) are $a = 7.1$ mm, $b = 1.6$ mm, $c = 1.8$ mm, $d = 2.2$ mm and $w_o = 1.5$ mm. The EM simulated transmission response of Figure 3(a) is in Figure 3(b), and this unit DGS section can provide the desired cutoff and attenuation pole frequency values. The cutoff frequency of the filter is 10.26 GHz, and the transmission zero occurs at 14.85 GHz. As seen in Figure 3(b), wide stopband bandwidth is achieved by using the H-shaped DGS. The equivalent circuit of the H-shaped DGS can be modeled as a parallel LC circuit as shown in Figure 3(c). Depending on the size and shape of the etched lattice, an attenuation pole can be generated by the combination of inductance and capacitance elements. By employing the proposed etched lattice, the effective permittivity and thereby the reactance of the microstrip line are increased.



Compact Stepped Impedance Lowpass Filter with wide Stopband

Figures 5(a) and 5(b) show the top and bottom views of the proposed lowpass filter, named as Filter-1, which consists of two symmetric H-shaped DGSs etched on the ground metallic plane of the basic lowpass filter structure. Two H-shaped units in the ground plane are separated by the spacing, $s = 4.1$ mm. The stopband bandwidth of the filter is improved by the use of etched units in the ground plane without increasing the physical size. The introduced H-shaped DGS units allow good selectivity and wide stopband bandwidth up to 20 GHz at 18 dB suppression level. The simulated 3 dB cutoff frequency of Filter-1 is 1.945 GHz, and wide stopband bandwidth from 2.315 GHz to 20 GHz with rejection level of 18 dB is achieved. The selectivity of the filter is 42.71 dB/GHz at 20 dB suppression level. The insertion loss is lower than 0.3 dB up to 1.1 GHz of the passband,

and the return loss is higher than 30.4 dB.



To improve the characteristics of Filter-1, one more H-shaped slot is added to the ground plane, and the coupling between the DGS resonators is increased. The new filter, Filter-2, is designed using the same FR4 substrate, which is used in Filter-1. Filter-2 offers improved passband and stopband characteristics as compared to that of Filter-1 without changing its normalized circuit size. Figures 7(a) and 7(b) show the top and bottom views of Filter-2. Due to the addition of one more H-shaped slot of different dimension, the effective permittivity and coupling between DGS resonators are increased. The proposed Filter-2 is designed.. The dimensions of the newly added H-shaped slot are $a1 = 8.6$ mm, $b1 = 1.5$ mm, $c1 = 2.8$ mm, $d1 = 2$ mm and $s1 = 0.35$ mm.

CHAPTER 4

RESULTS AND DISCUSSION

i).Dual split resonator lowpass filter with ultrawide stopband and sharp roll-off rate

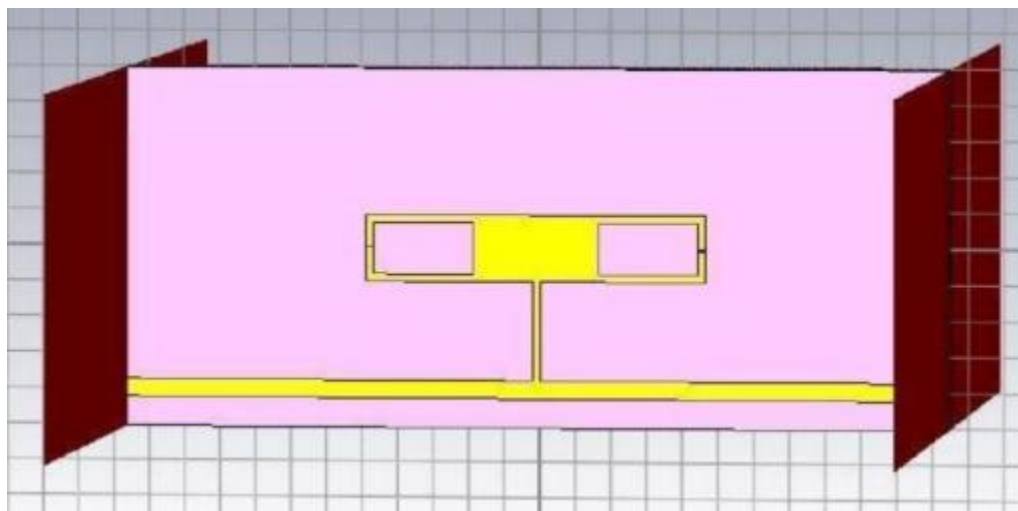


Fig 4.1. Structure of DSR1

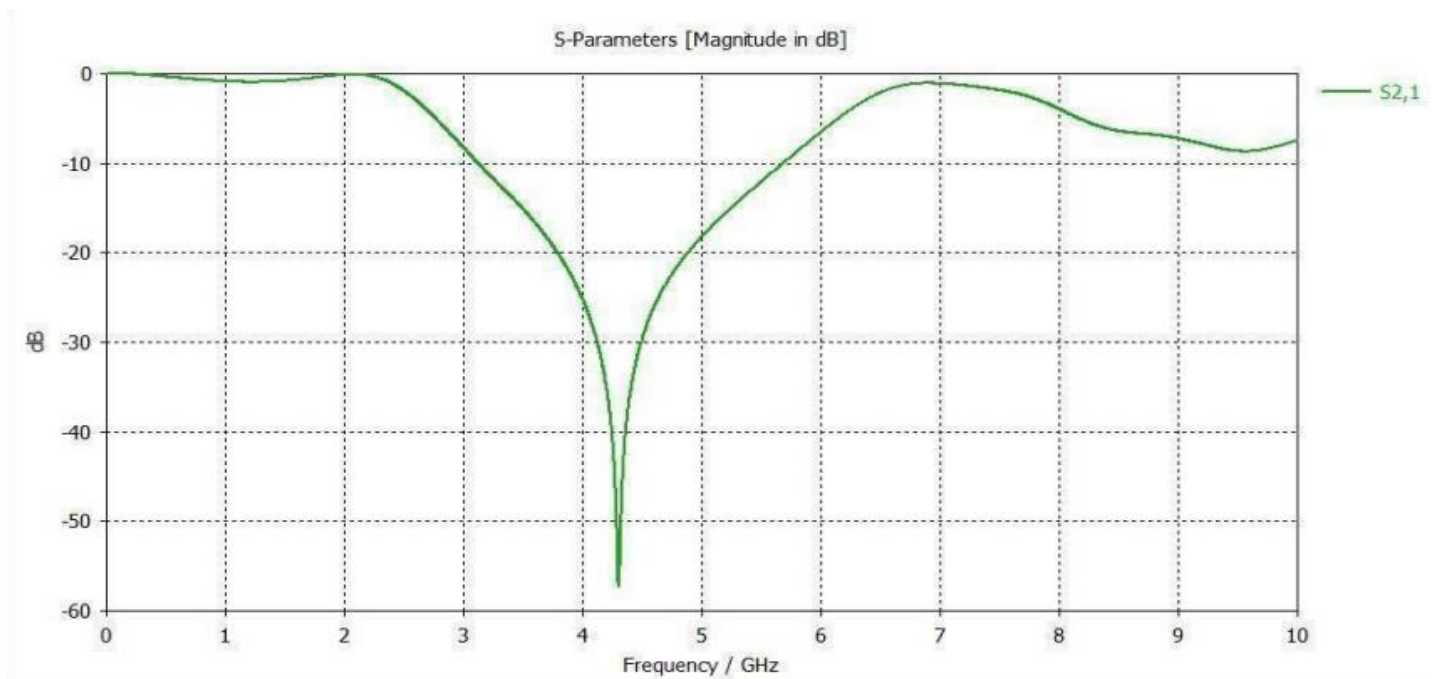


Fig 4.2.Simulation results of DSR1

The 3dB cutoff frequency occurs at 2.46GHz.DSR-1 resonates at 4.3 GH

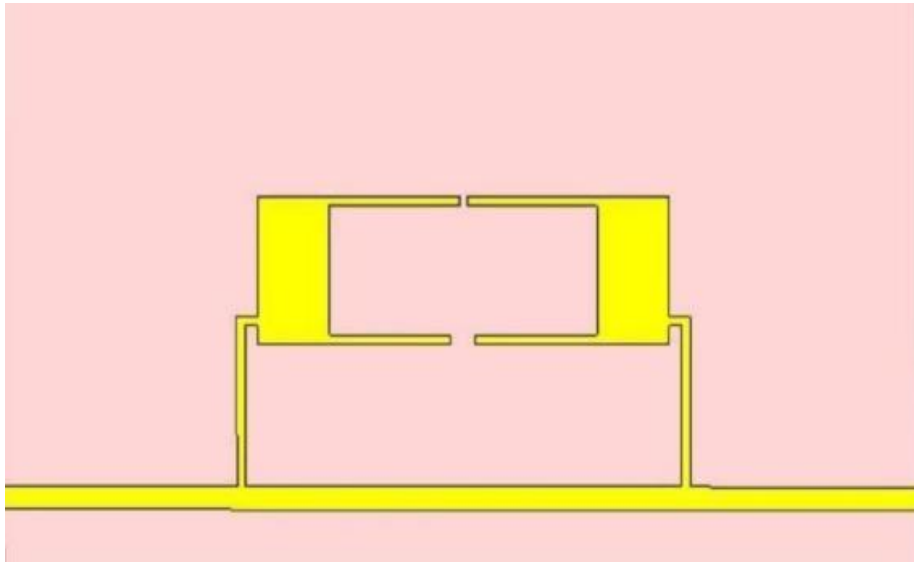


Fig 4.3. Structure of DSR2

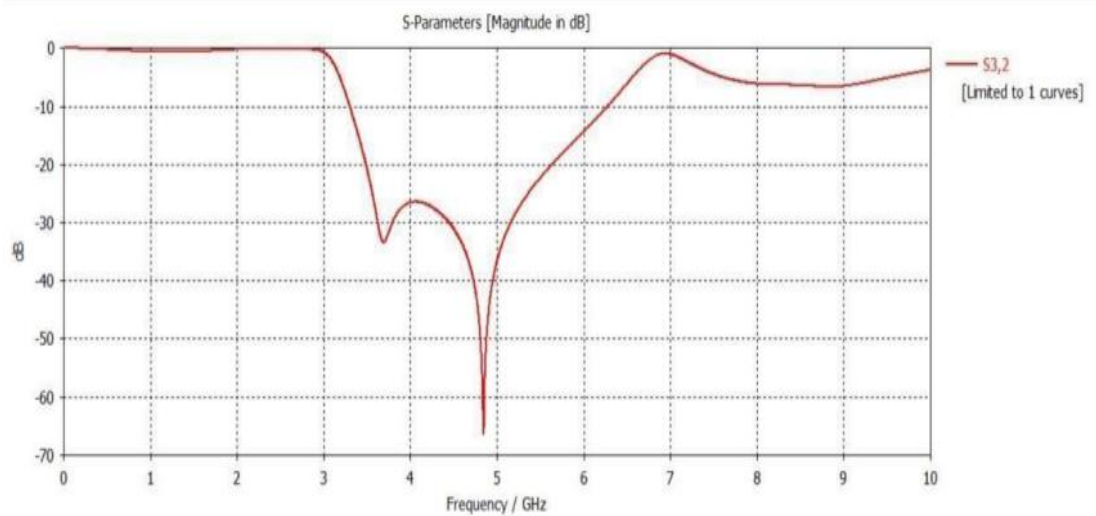


Fig.4.4 Simulated results of DSR2

The DSR2 simulated with two resonators on each side have two resonant frequencies f_{z1} and f_{z2} with 35 and 65dB attenuation at 3.7GHz and 4.8GHz.

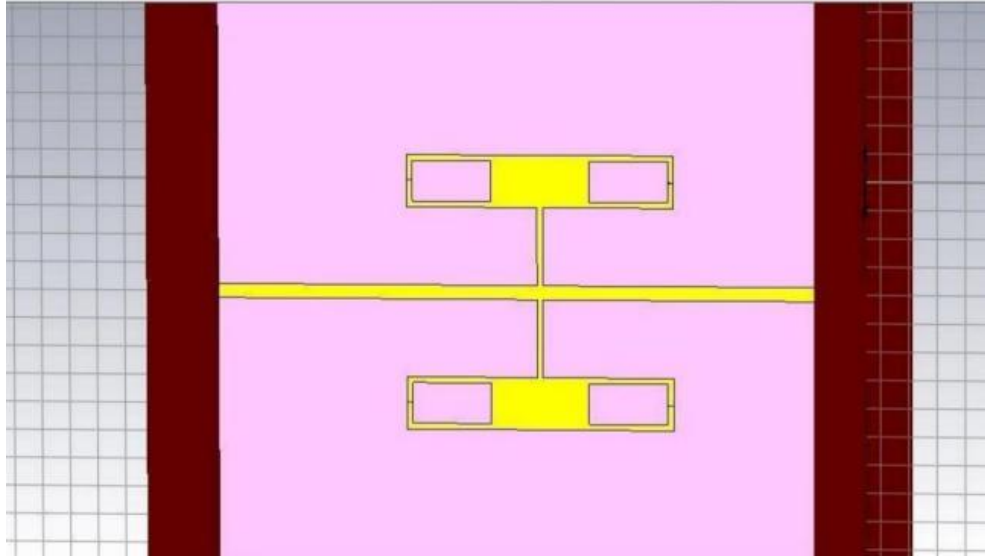


Fig.4.4 Structure of two DSR1 connected

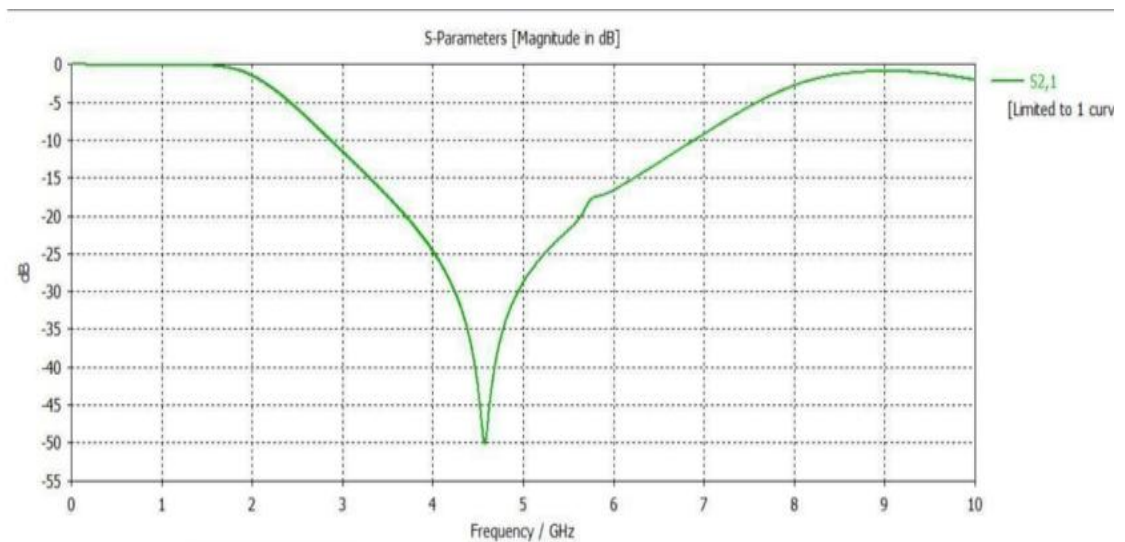
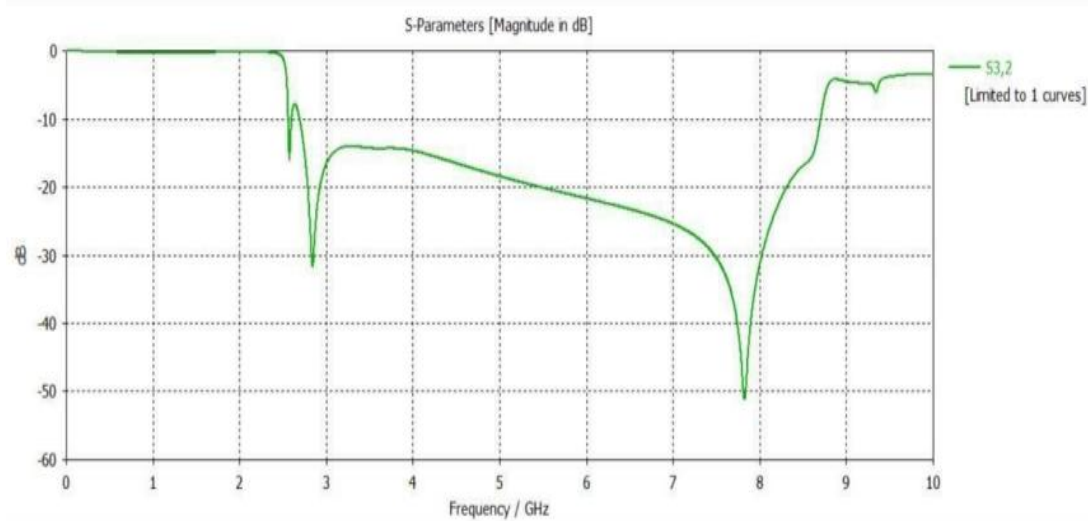
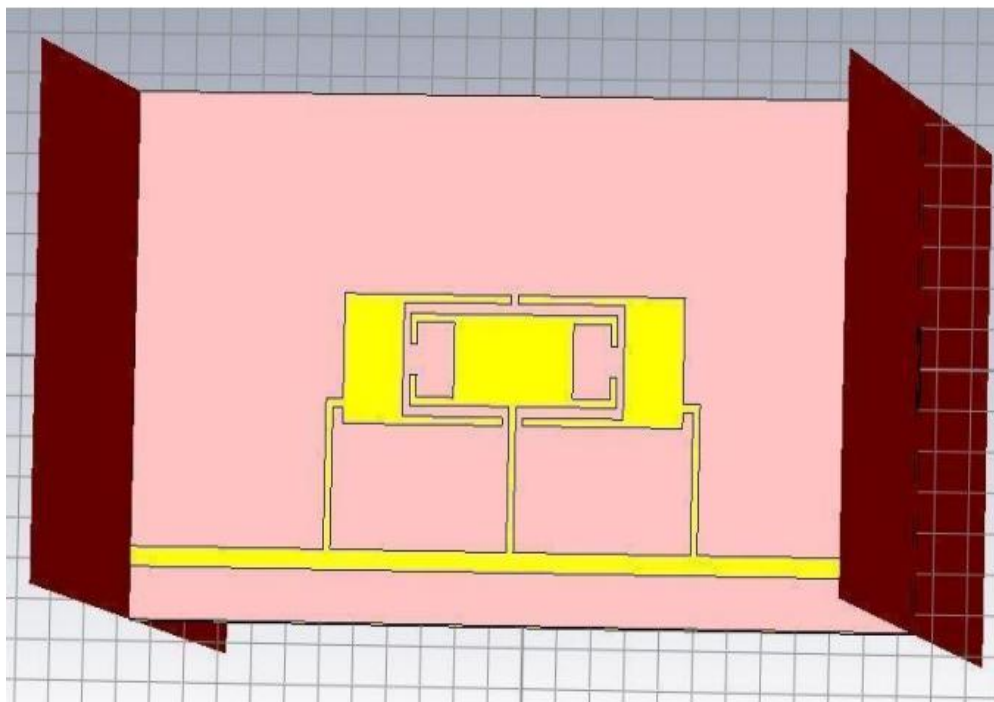
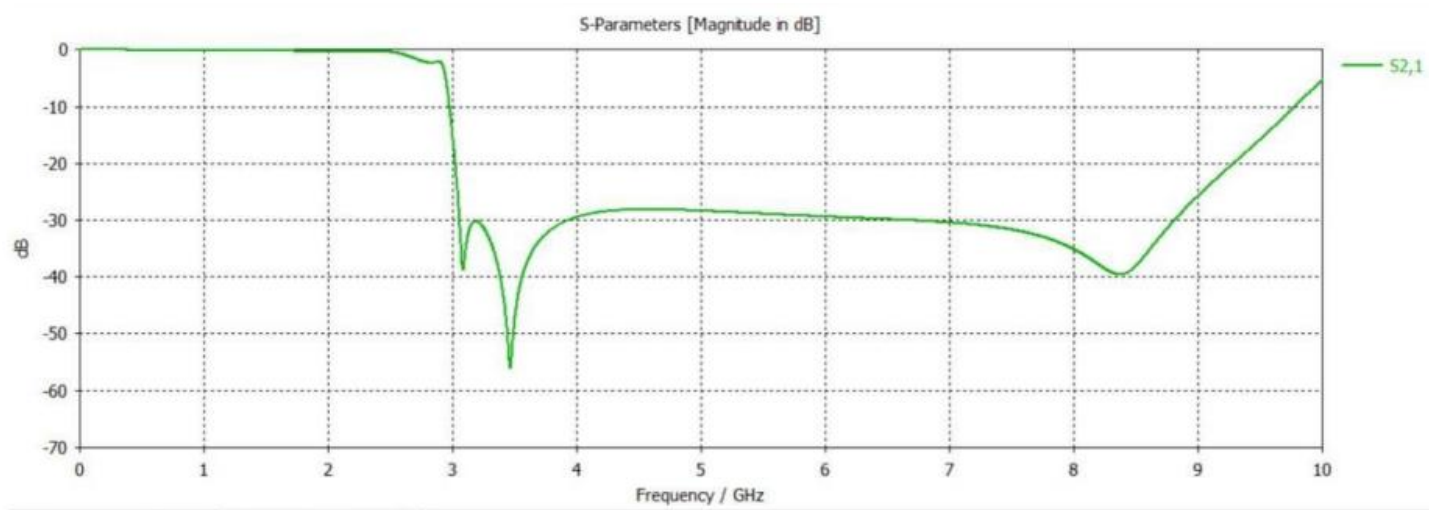
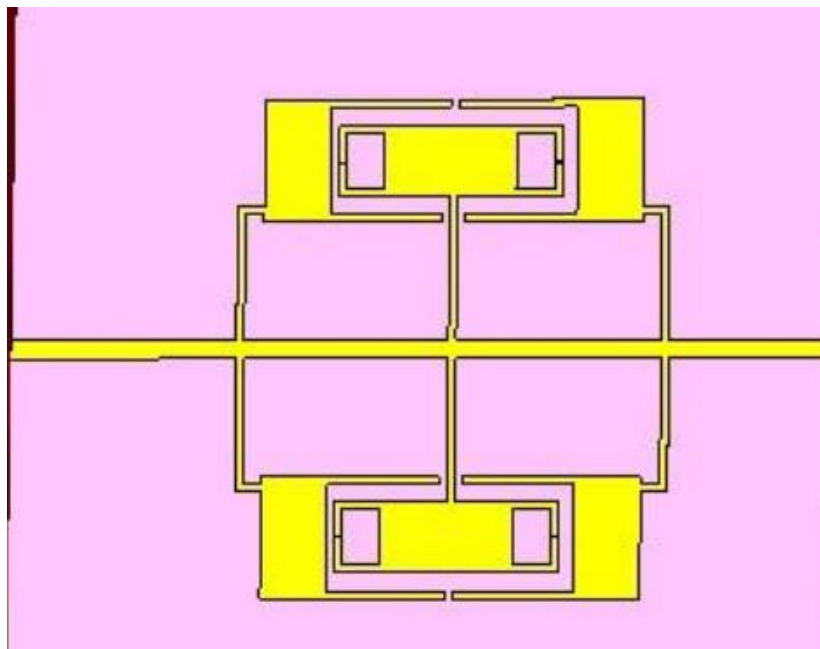
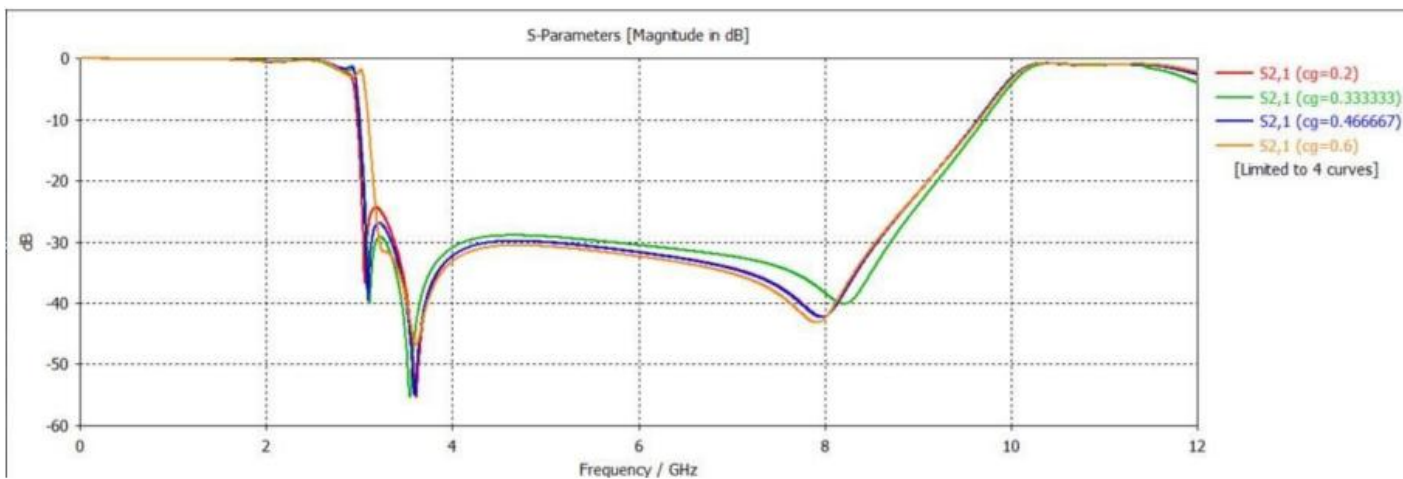
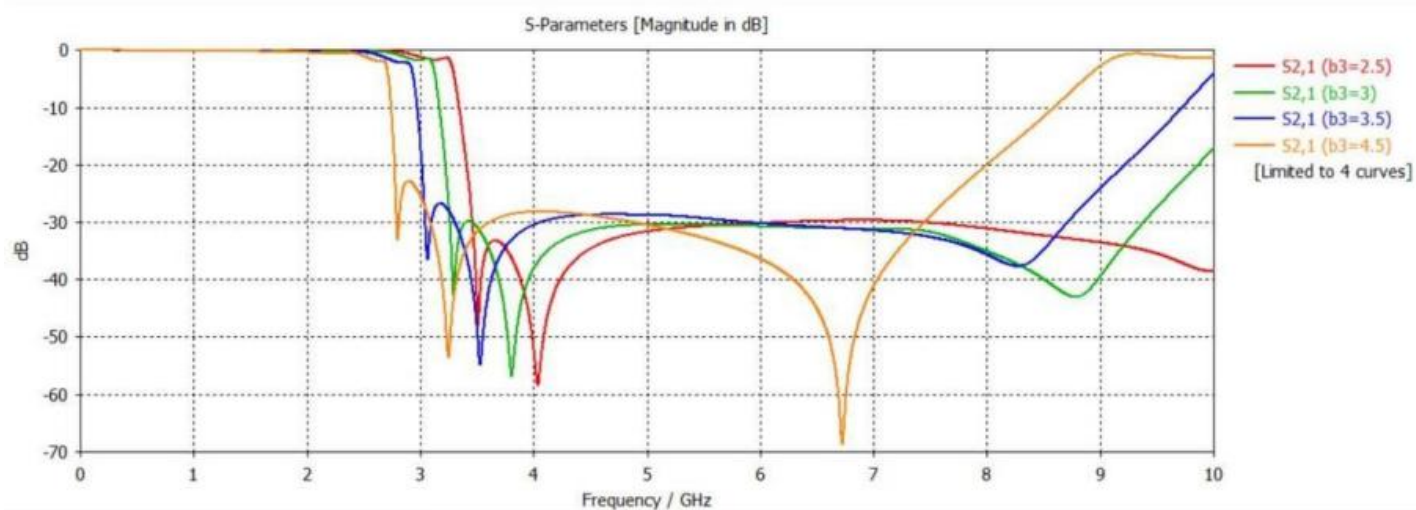
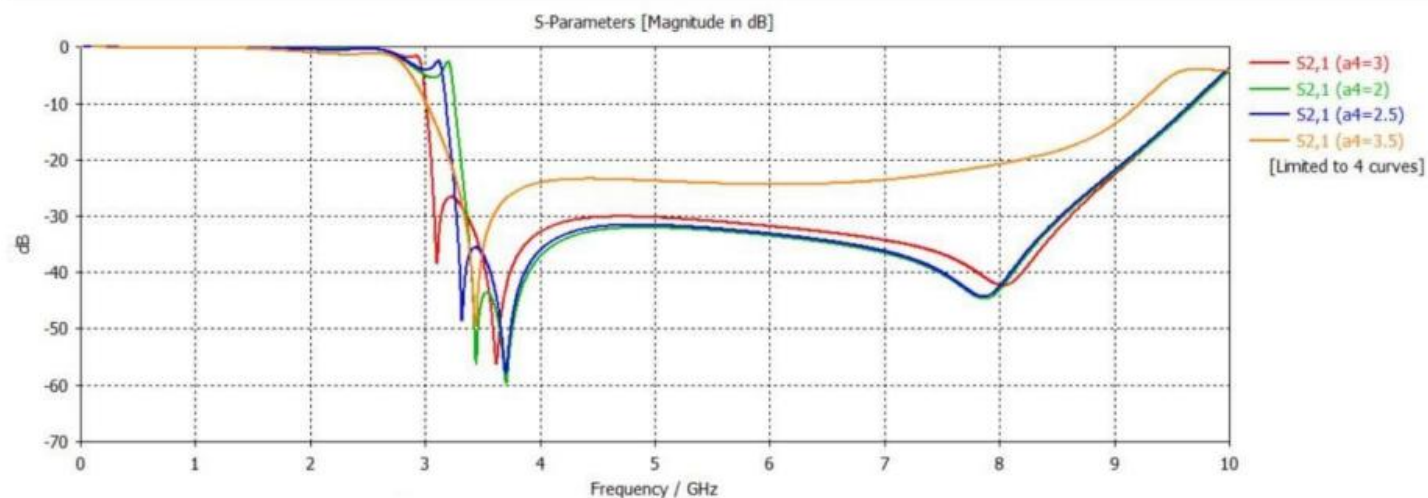


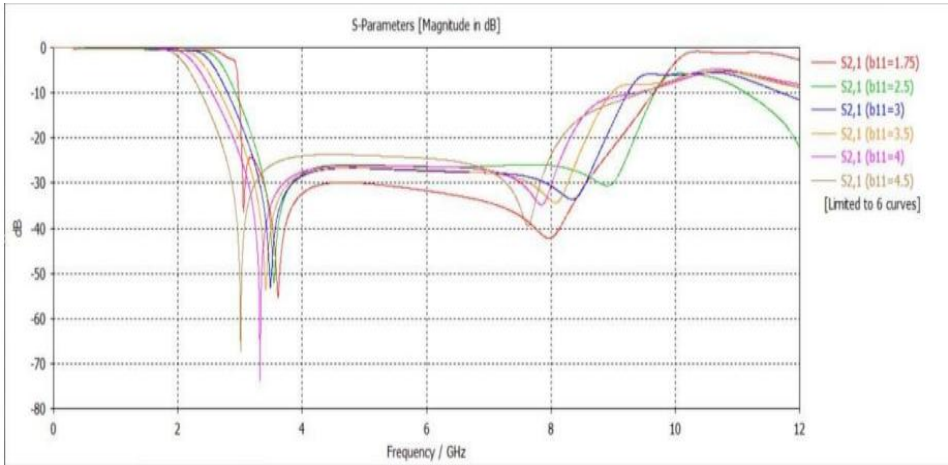
Fig.4.4 Simulated results of two DSR1 connected

By using the single DSR-1 in Section 1 and symmetrical DSR-1 in Section 2, there is no significant variation in the position of transmission zero, but the cut-off frequency is reduced from 3.1 to 2.5 GHz









Capacitively-Coupled Resonators for Terahertz Planar-Goubau-Line Filters

The experimental findings of the study provide comprehensive insights into the performance and behavior of the fabricated planar Goubau line (PGL) filter, elucidating its efficacy in terahertz (THz) frequency applications.

Loss Characteristics: Initially, the measured S-parameters of a 1-mm-long PGL devoid of resonators were presented in Fig., revealing a loss ranging from 1 dB/mm at 0.5 THz to 3 dB/mm at 1.1 THz. Remarkably, these losses signify relatively low attenuation for a metal planar waveguide operating at THz frequencies, with the magnitude of S11 hovering near the noise floor of the measurement setup.

Filter Performance: Fig. 9 showcases the measured S-parameters of the filter across the frequency spectrum of 0.5 to 1.1 THz, alongside corresponding 3-D simulations. Encouragingly, the results from electromagnetic simulations exhibit excellent concordance with experimental measurements, albeit minor disparities in S21 attributed to fabrication tolerances, material property variations, and calibration uncertainties. The transmission-line model effectively delineates the passband/stopband regime, albeit with a slight frequency shift, more pronounced at higher frequencies. The filter's S21 depicts a stopband and a passband centered at 0.6 THz and 0.9 THz, respectively, boasting 3-dB bandwidths of 27% and 31%. Despite exhibiting an insertion loss of 7 dB for the passband, approximately 4 dB higher than a resonator-free PGL of identical length, the filter remains competitive compared to planar filters in the submillimeter band. Notably, both S11 and S21 exhibit asymmetrical passband responses, characterized by steeper band transitions at higher passband frequencies, likely influenced by an increase in the effective refractive index induced by periodic resonators.

The results underscore the effectiveness of the proposed PGL filter design, demonstrating favorable performance characteristics across the desired frequency range. Despite minor disparities between simulations and measurements, the filter exhibits competitive insertion loss and bandwidth, making it suitable for practical THz applications. The observed asymmetry in passband responses and ripple effects in S_{11} highlight the complexities inherent in designing and characterizing THz filters, warranting further investigation into optimizing filter designs and fabrication processes to minimize such effects. Overall, the results affirm the feasibility of employing periodic $\lambda/2$ resonators in PGL filters, offering insights into their operating principles and potential for realizing high-performance

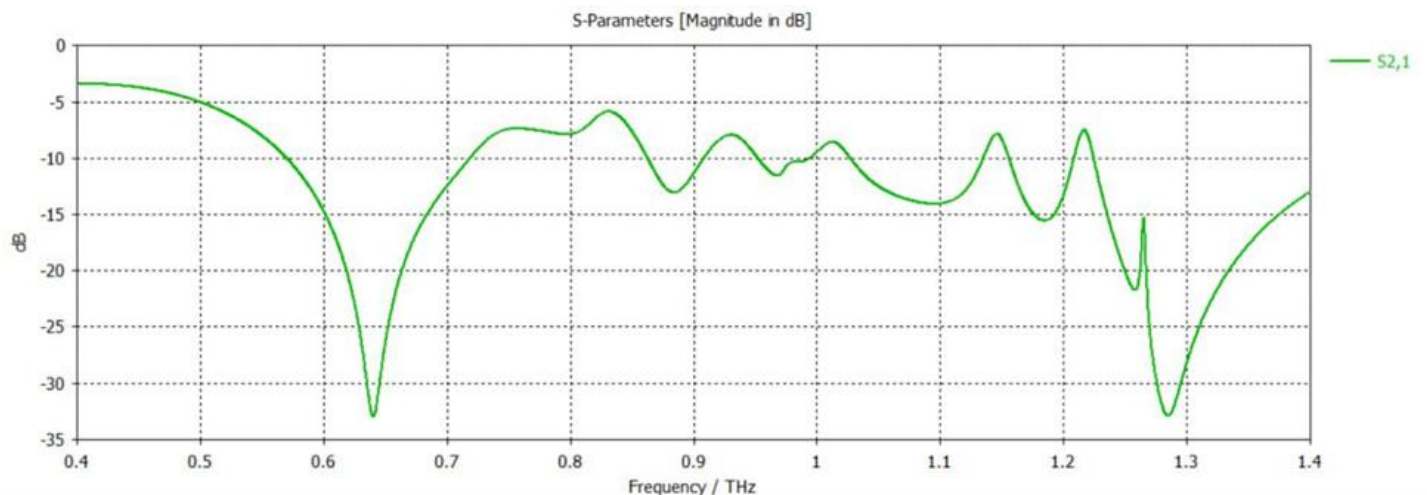
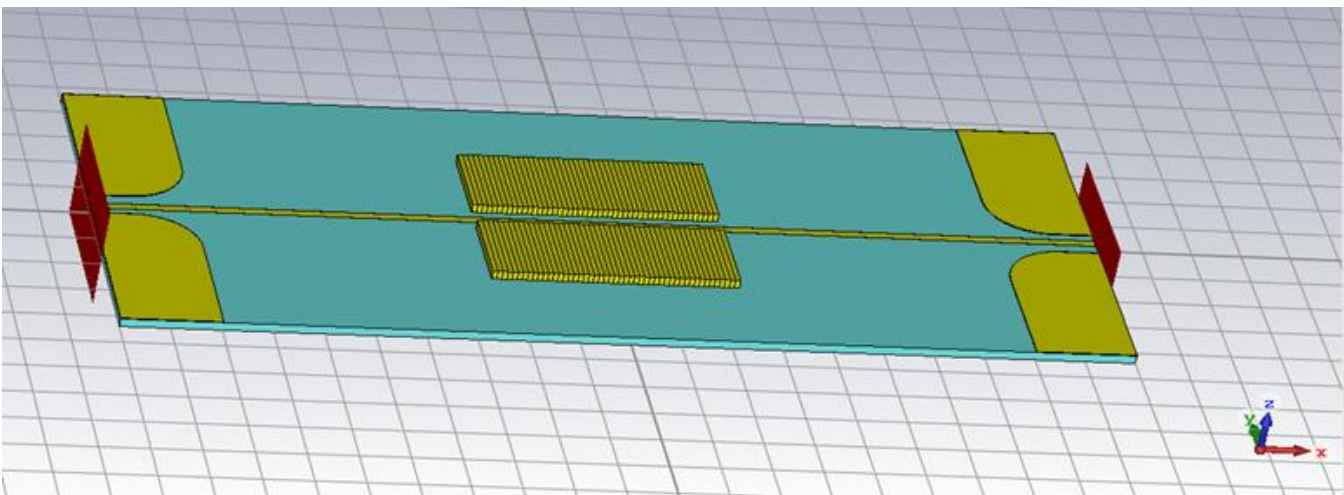
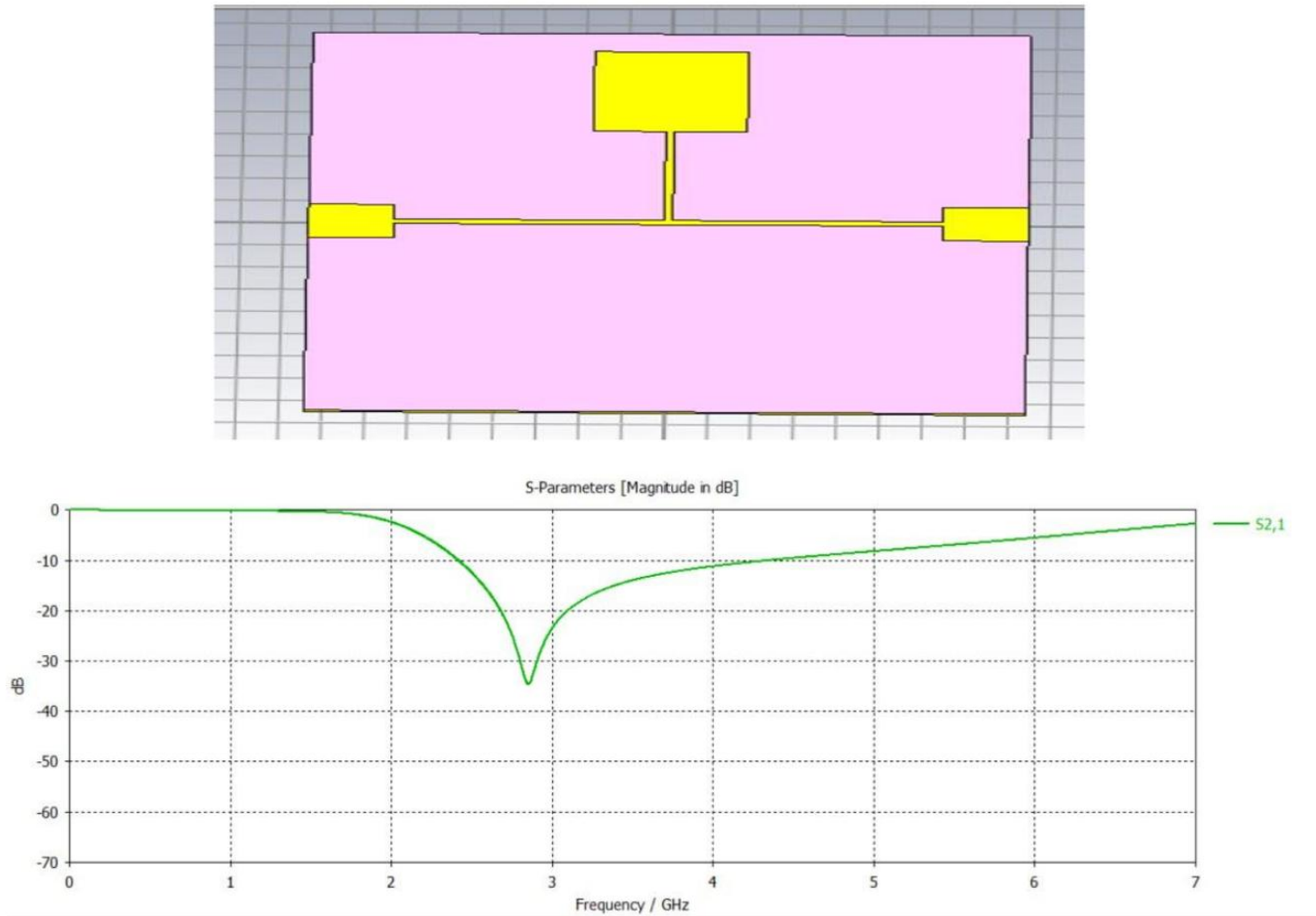
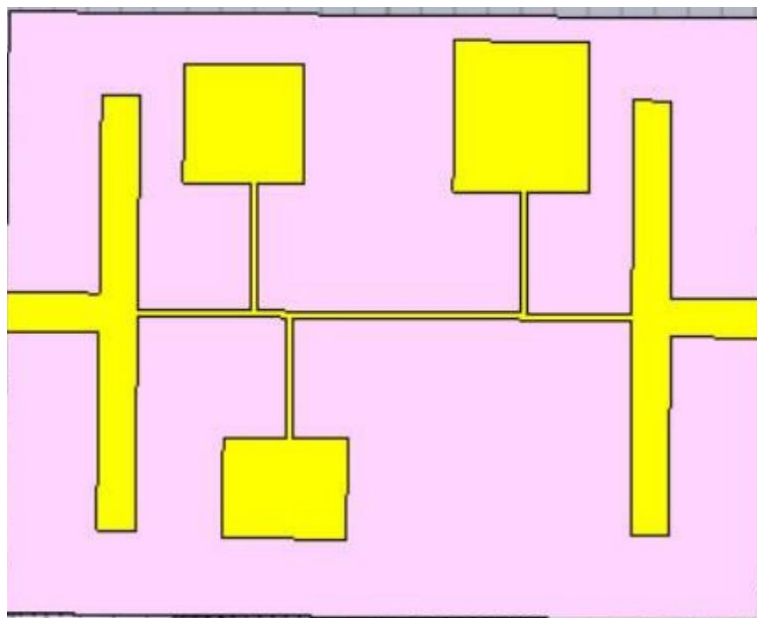
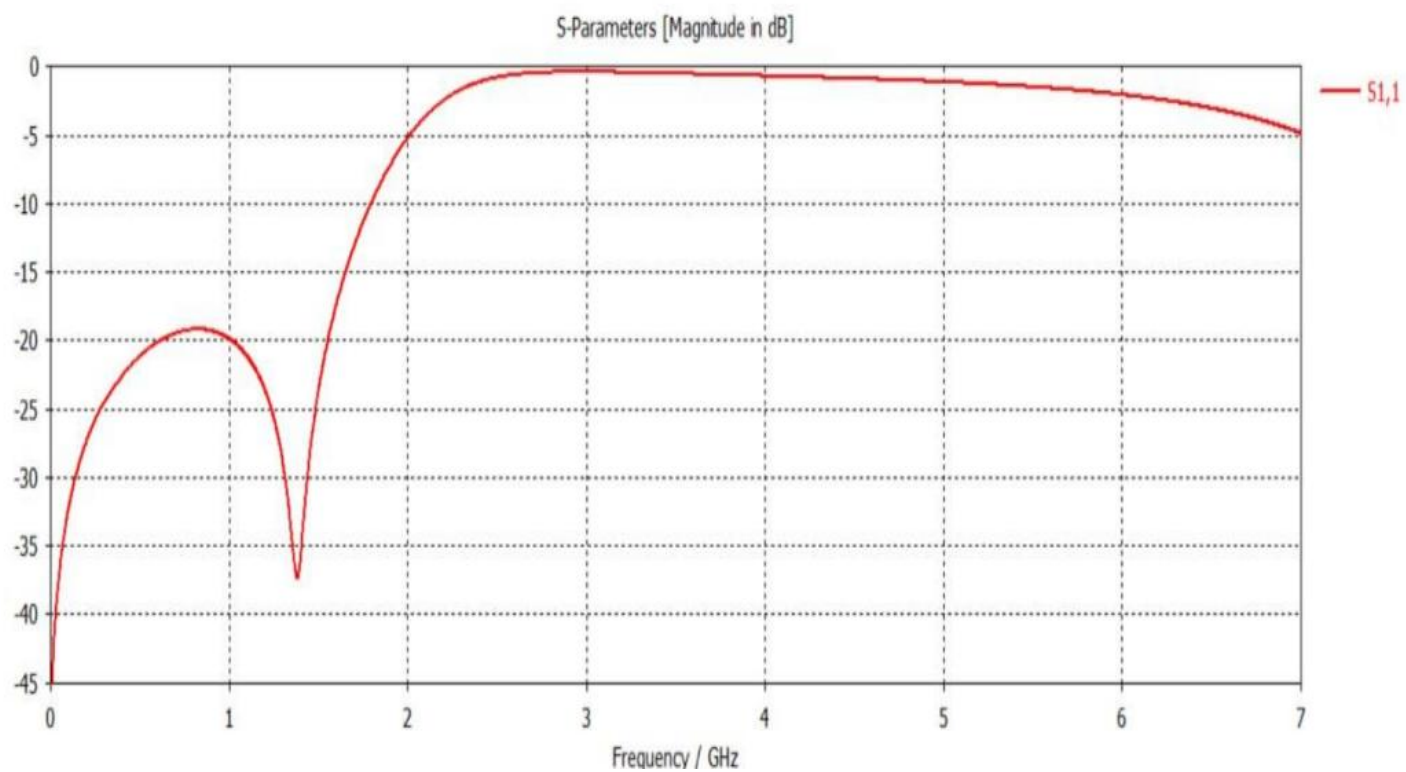
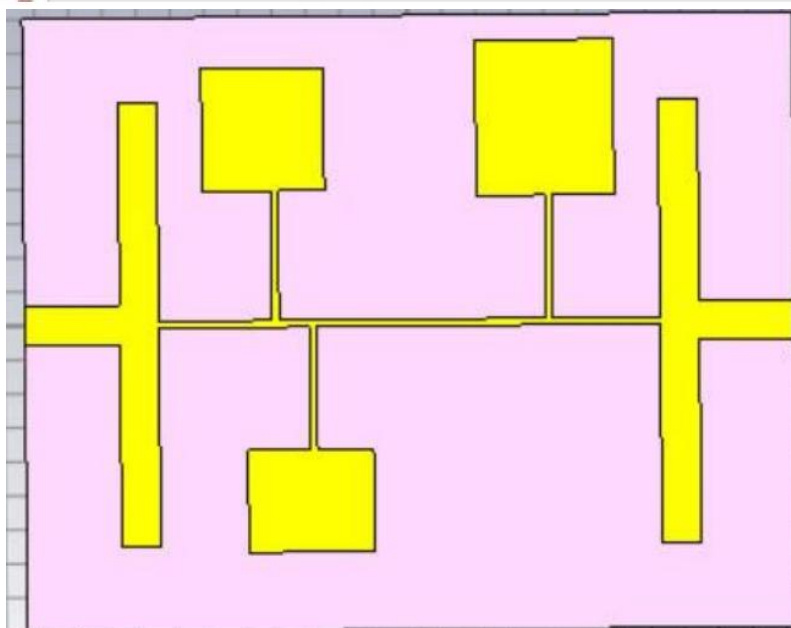
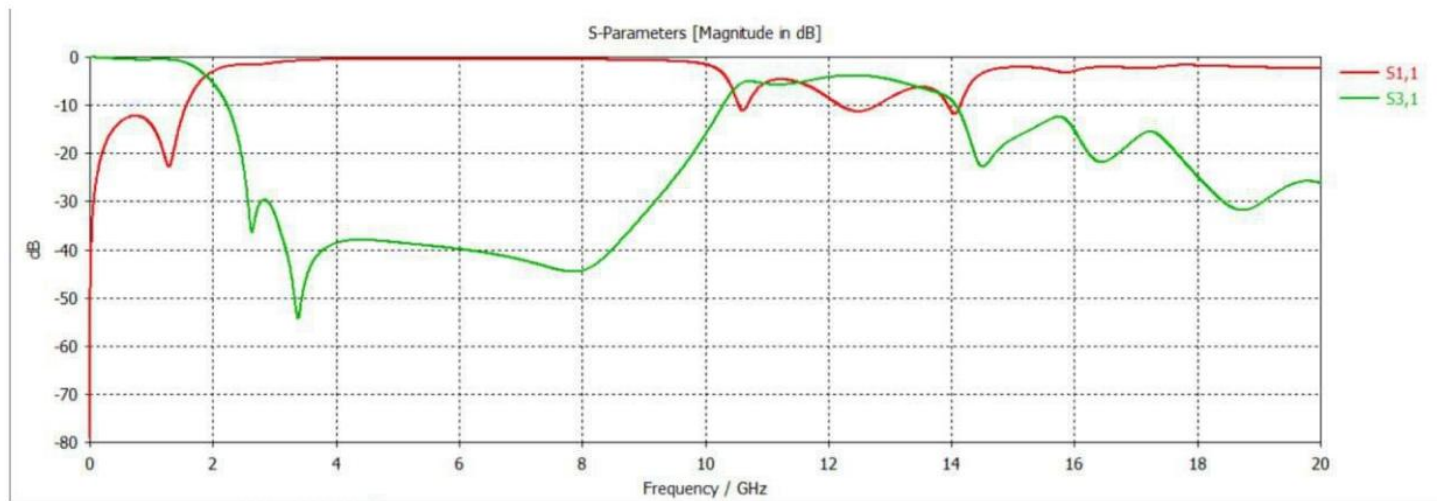


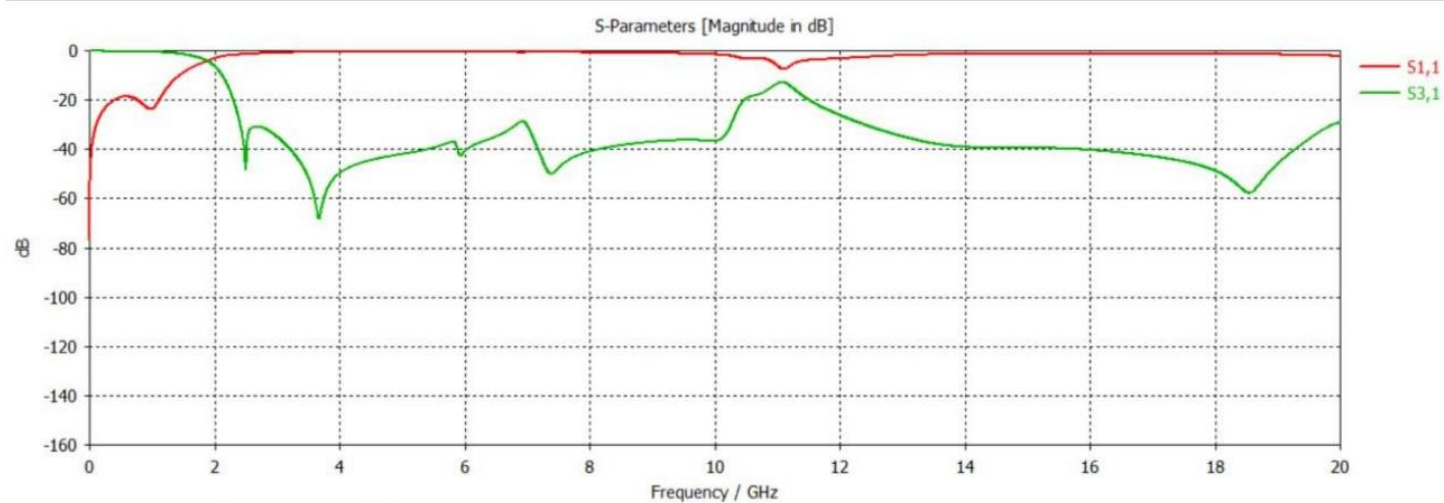
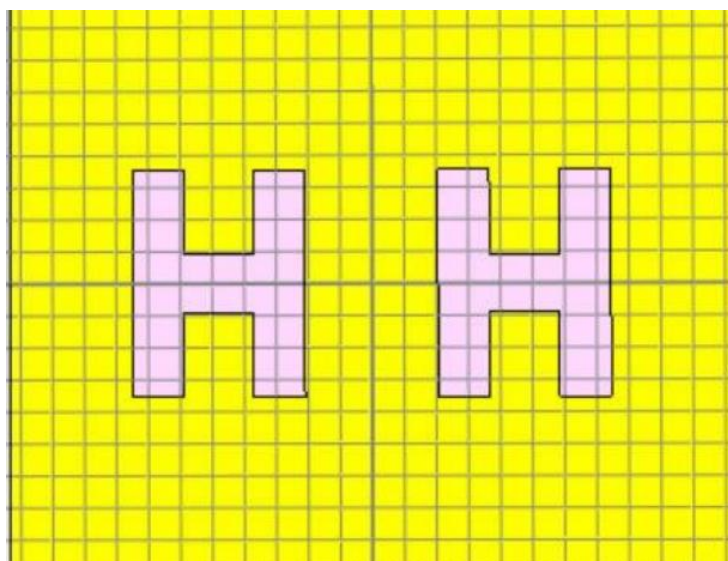
Fig: Simulation results of Capacitively coupled resonators for Terahertz Planar Goubau Line filters

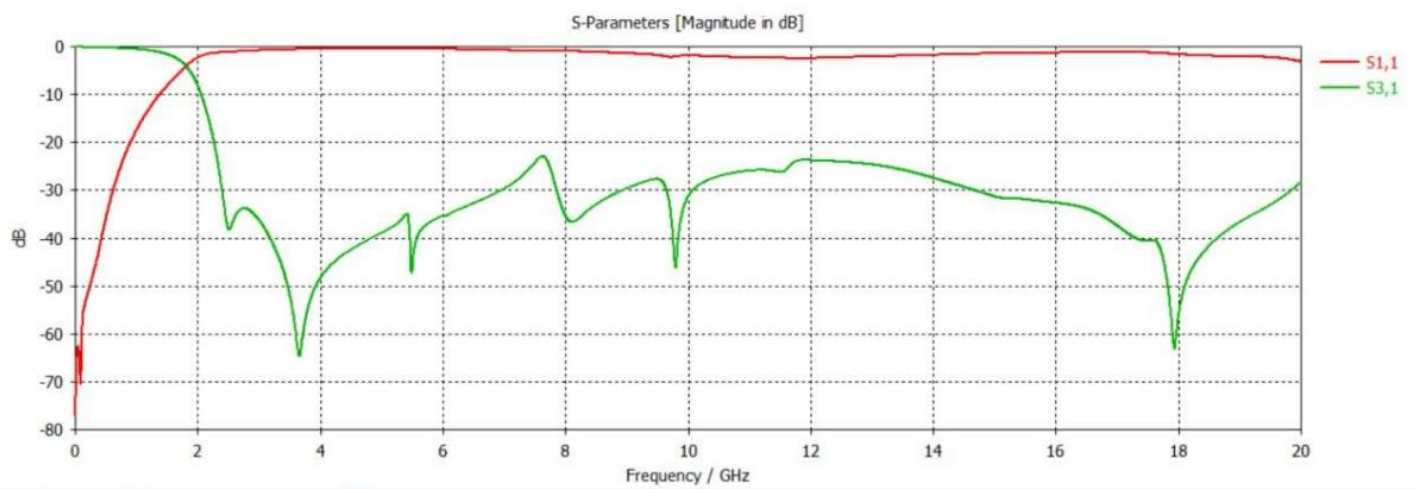
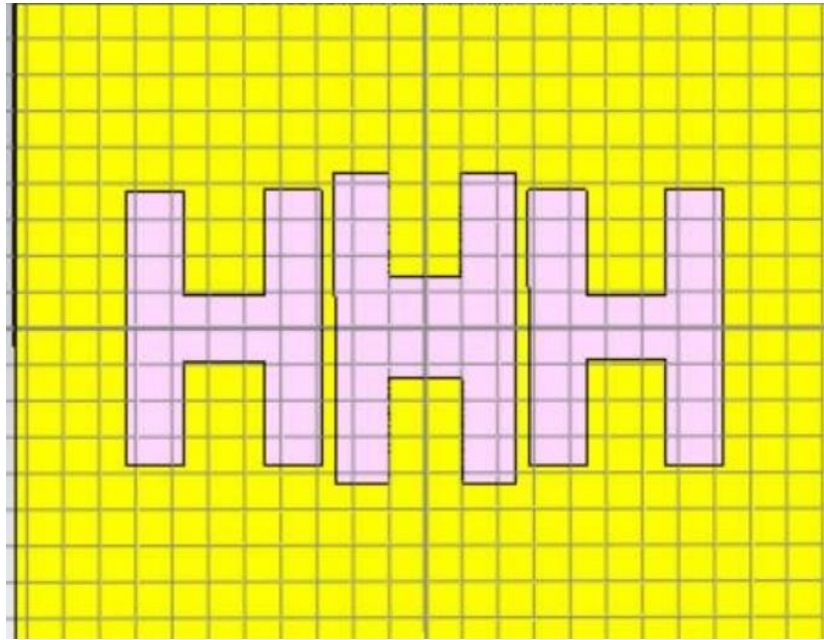
ii).Improved Frequency Response of Microstrip Lowpass Filter Using Defected Ground Structures











CHAPTER 4

CONCLUSION AND FUTURE PROSPECTS

In conclusion, the study of Gigahertz (GHz) and Terahertz (THz) filters has revealed promising advancements in microwave engineering. Researchers have extensively explored various designs, including Split Ring Resonators (SRRs), Complementary Split Ring Resonators (CSRRs), and Dual Split Resonators (DSRs), to enhance filter performance. The development of novel geometries and structures, such as dual splits in resonators, has shown significant improvements in filter response characteristics, such as roll-off rate and stopband suppression. Looking ahead, the future of GHz and THz filters appears promising, with continued efforts focused on refining design methodologies, exploring new materials, and pushing the frequency boundaries to address emerging applications in wireless communication, radar systems, sensing, and imaging. Additionally, advancements in fabrication techniques, such as additive manufacturing and nanofabrication, offer opportunities for creating more compact, efficient, and cost-effective filter solutions. Overall, the evolution of GHz and THz filters is poised to play a crucial role in enabling next-generation wireless technologies and applications in the years to come. In addition to the current advancements, the future prospects for Gigahertz (GHz) and Terahertz (THz) filters are promising as researchers delve deeper into cutting-edge technologies and applications. One significant avenue is the exploration of novel materials and fabrication techniques tailored for GHz and THz frequencies. Researchers are investigating metamaterials, graphene, and other nanomaterials to

achieve unprecedented filter performance, including ultra-compact size, low insertion loss, and high selectivity. Moreover, the integration of GHz and THz filters into emerging technologies such as 5G networks, Internet of Things (IoT), and beyond offers vast opportunities for innovation. These filters will play a critical role in enabling higher data rates, improved spectral efficiency, and enhanced connectivity in wireless communication systems. Additionally, GHz and THz filters hold promise for applications in advanced radar systems, biomedical imaging, security screening, and environmental sensing. Furthermore, advancements in design optimization algorithms, simulation tools, and characterization techniques will accelerate the development and deployment of GHz and THz filters. Machine learning and artificial intelligence techniques are increasingly being applied to optimize filter designs, predict performance characteristics, and automate the design process, leading to faster prototyping and commercialization.

REFERENCES

- 1. Dual split resonator lowpass filter with ultrawide stopband and sharp roll-off rate: IET Microwaves, Antennas & Propagation Research Article: Thevaruparambil Abdulnazer Nisamol¹, Parambil Abdulla¹, Paruthikkal M. Raphika² ¹Division of Electronics, School of Engineering, Cochin University of Science and Technology, Cochin 682022, India ²Department of Electronics, MES College Marampally, Kerala, India.*
- 2. Design of Low Pass Filter using Microstrip Line, publisher: IEEE - A Comparative Study*

APPENDICES

1. <https://youtu.be/bbePoHzv1B8?si=fdH-peMmAfe44AMK>
2. <https://youtu.be/vFQeJHqyPoU?si=dzeiq6kH5v9bkLei>
3. <https://youtu.be/3H451gzv84c?si=7COxdFZHClSZh0Bj>

